1 Introduction

1.1 The X-Ray and Extreme Ultraviolet Regions of the Electromagnetic Spectrum

One of the last regions of the electromagnetic spectrum to be developed is that extending from the extreme ultraviolet to hard x-rays, generally shown as a dark region in charts of the spectrum. It is a region where there are a large number of atomic resonances, leading to absorption of radiation in very short distances, typically measured in nanometers (nm) or micrometers (microns, μm), in all materials. This has historically inhibited the pursuit and exploration of the region. On the other hand, these same resonances provide mechanisms for both elemental (C, N, O, etc.) and chemical (Si, SiO_2, $TiSi_2$) identification, creating opportunities for advances in both science and technology. Furthermore, because the wavelengths are relatively short, it becomes possible to study nanoscale structures using the techniques of absorption, scattering and microscopy. To exploit these opportunities requires advances in relevant technologies, for instance in nanofabrication. These in turn lead to new scientific understandings, in subjects such as materials science, surface science, chemistry, biology and physics, providing feedback to the enabling technologies. Development of the extreme ultraviolet, soft and hard x-ray spectral regions is presently in a period of rapid growth and interchange among science and technology.

Figure 1.1 shows that portion of the electromagnetic spectrum extending from the infrared to the x-ray region, with wavelengths across the top and photon energies along the bottom. Major spectral regions shown are the infrared (IR), which we associate with molecular resonances and heat; the visible region from red to violet, which we associate with color and vision; the ultraviolet (UV), which we associate with sunburn and ionizing radiation; the regions of extreme ultraviolet (EUV), soft x-rays (SXR), and finally hard x-rays, which we associate with medical and dental x-rays and with the scientific analysis of crystals, materials, and biological samples through the use of diffraction, scattering, and other techniques. In this book we address techniques and opportunities based on the generation and use of radiation extending from the EUV through x-ray regions of the spectrum.

The extreme ultraviolet is taken here as extending from photon energies of about 30 eV to about 250 eV, with corresponding wavelengths in vacuum extending from

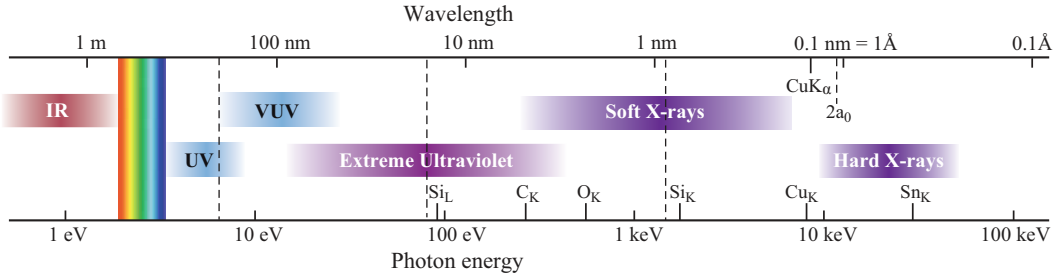

- See smaller features
- Write smaller patterns
- Elemental and chemical sensitivity
- Penetrate visibly opaque objects

Figure 1.1 The electromagnetic spectrum as it extends from the infrared (IR) to the x-ray regions. Visible light is shown with red (650 nm), green (530 nm), and blue (470 nm) wavelengths. At shorter wavelengths are ultraviolet (UV) radiation, extreme ultraviolet radiation (EUV), soft x-rays (SXR), and hard x-rays. Shown for reference are the silicon L-absorption edge at 99.2 eV (12.5 nm wavelength), the carbon K-absorption edge at 284 eV (4.37 nm), the oxygen K-absorption edge at 543 eV (2.28 nm), the silicon K-absorption edge at 1.84 keV (0.674 nm), the copper K-absorption edge at 8.98 keV (1.38 Å), the tin K-absorption edge at 29.2 keV (0.423 Å), the copper K_α-emission line at 1.54 Å (8.05 keV), and twice the Bohr radius at $2a_0 =$ 1.06 Å, the diameter of the $n = 1$ orbit in Bohr's model of the hydrogen atom, but more generally a dimension within which resides most of the charge for all atoms. Vertical dashed lines correspond to the transmission limits of common window materials used to isolate vacuum. Shown are approximate transmission limits for common thicknesses of fused silica (pure SiO_2) at 200 nm, a thin film of silicon nitride (~100 nm thick Si_3N_4) at 15 nm, and an 8 μm thick beryllium foil at a wavelength of about 1 nm.

about 5 nm to 40 nm.* The soft x-ray region is taken as extending from about 250 eV (just below the carbon K-edge) to several keV, and the x-ray region of interest here extends from photon energies just below 10 keV to energies approaching 100 keV, all as shown in Figure 1.1. These spectral regions are characterized by the presence of the primary atomic resonances and absorption edges of most elements, from low to high Z, where Z is the atomic number (the number of protons in the nucleus). The primary atomic absorption edges† for selected elements are given in Table 1.1, along with $1/e$ absorption lengths at photon energies of 100 eV, 1 keV, and 10 keV. The K- and L-absorption edges, associated with the removal of a core electron by photoabsorption from the most tightly bound atomic states (orbitals of principal quantum numbers $n =$ 1 and $n = 2$, respectively), are described later in this chapter. The K-absorption edges of carbon (C_K), oxygen, silicon, copper and tin are shown in Figure 1.1, as is the L-absorption edge of silicon (Si_L), just below 100 eV.

* It is common to express photon energies in this spectral region in electron volts (eV) or thousands of electron volts (keV), where the photon energy is $\hbar\omega$, $\hbar$ is Planck's constant divided by 2π, and $\omega = 2\pi f$ is the radian frequency. Wavelengths (λ) are commonly expressed in nanometers (1 nm = 10^{-9} m) and ångströms (1 Å = 10^{-10} m). See Appendix A for the values of physical constants and conversion factors.

† Standard reference data for this spectral region are given in Refs. 1–4.

Table 1.1 K- and L_3-absorption edges for selected elements. Also given are $1/e$ absorption depths at photon energies of 100 eV, 1 keV, and 10 keV. Energies are given to the nearest electron volt. They are measured from the vacuum level for gases (N_2, O_2), relative to the Fermi level for metals, and relative to the top of the valence band for semiconductors. Wavelengths are given to three significant figures. These K- and L-edge values can vary somewhat with the chemical environment of the atom. Values here are taken from Williams.[1] Absorption lengths are obtained from Henke, Gullikson, and Davis.[3]

						l_{abs}		
Element	Z	K_{abs}-edge (eV)	L_{abs}-edge (eV)	$\lambda_{K\text{-abs}}$ (nm)	$\lambda_{L\text{-abs}}$ (nm)	100 eV (nm)	1 keV (μm)	10 keV (μm)
Be	4	112	–	11.1	–	730	9.0	9600
C	6	284	–	4.36	–	190	2.1	2100
N	7	410	–	3.02	–	–	–	–
O	8	543	–	2.28	–	–	–	–
H_2O						160	2.3	2000
Al	13	1560	73	0.795	17.1	34	3.1	160
Si	14	1839	99	0.674	12.5	63	2.7	130
S	16	2472	163	0.502	7.63	330	1.9	100
Ca	20	4039	346	0.307	3.58	290	1.3	69
Ti	22	4966	454	0.250	2.73	65	0.38	20
V	23	5465	512	0.227	2.42	46	0.26	14
Cr	24	5989	574	0.207	2.16	31	0.19	10
Fe	26	7112	707	0.174	1.75	22	0.14	7.4
Ni	28	8333	853	0.149	1.45	16	0.11	5.4
Cu	29	8979	933	0.138	1.33	18	0.10	5.1
Se	34	12 658	1434	0.0979	0.865	63	0.96	52
Mo	42	20 000	2520	0.0620	0.492	200	0.19	12
Sn	50	29 200	3929	0.0425	0.316	17	0.17	11
Xe	54	34 561	4782	0.0359	0.259	–	–	–
W	74	69 525	10 207	0.0178	0.121	28	0.13	5.6
Au	79	80 725	11 919	0.0154	0.104	28	0.10	4.5

We see in Table 1.1 that many of these absorption edges lie in the combined x-ray and extreme ultraviolet spectral region. What differentiates these regions from neighboring spectral regions is the high degree of absorption in all materials. At lower photon energies, in the visible and ultraviolet, and at higher photon energies, well into the hard x-ray region, many materials become transparent and it is not necessary to utilize vacuum isolation techniques. For example, Figure 1.1 shows dashed vertical lines at the locations of common window materials that can hold vacuum over square centimeter areas while still transmitting radiation in the indicated regions. In the UV, fused silica, a form of pure SiO_2, is transmissive to wavelengths as short as 200 nm, in millimeter thicknesses. For shorter wavelengths one quickly enters the vacuum ultraviolet (VUV), where air and all materials are absorbing. Shown just below 1 nm wavelength is the transmission limit of a thin ($\cong$8 μm) beryllium foil that transmits photons of energy greater than about 1.5 keV. For many years these two materials defined the limits of available window materials. More recently thin films ($\sim$100 nm) such as silicon nitride

(stoichiometrically Si_3N_4) have extended transmissive windows to photon energies just under 100 eV, as shown in Figure 1.1.

While this plenitude of atomic resonances and efficient photoabsorption has made the EUV and soft x-ray regions more difficult to access, it also provides a very sensitive tool for elemental and chemical identification, thus creating many scientific and technological opportunities. These opportunities are enhanced in this spectral region in that the wavelengths are short, but not so short as to preclude the development of high-resolution optical techniques, thus permitting direct image formation and spatially resolved spectroscopies, to spatial resolutions of order 10 nm. The relative transparency of water and its natural contrast with other elements further add to these opportunities, for instance for spectroscopy and imaging in the life and environmental sciences.

In the paragraphs that follow we will briefly review the basic processes of absorption, scattering, and photoemission; atomic energy levels and allowed transitions; and associated absorption edges and characteristic emission lines. We note two interesting features associated with wavelengths in the EUV/x-ray spectral region. In the EUV and soft x-ray regions the wavelengths are large compared to the Bohr radius, $\lambda \gg a_0$, where a_0 is the radius of the first ($n = 1$) stationary electron orbit in the Bohr model of hydrogen.[‡] More significantly here, the diameter $2a_0 = 1.06$ Å typically encompasses most of the electronic charge in multi-electron atoms,[¶] so that to a large degree the treatment of scattering in the EUV/SXR region simplifies as the various atomic electrons experience a rather uniform phase variation, an assumption that does not hold at shorter x-ray wavelengths. For the shorter wavelength, however, these same simplifications are valid for x-rays scattering into the forward direction, which contributes to refractive index. Furthermore, because the wavelengths of interest in this text are longer than the Compton wavelength[4, 5] ($\lambda \gg \lambda_C = h/mc = 0.0243$ Å), momentum transfer from the photon can be ignored during the scattering process, again simplifying analysis in the EUV/x-ray spectral region.

Finally, we close this section with some numerical relationships in units[7, 8] convenient for work in this spectral region. Based on the dispersion relation in vacuum, $f\lambda = c$ or $\omega = kc$, where c is the velocity of light[§] in vacuum and $\omega = 2\pi f$, the product of photon energy $\hbar\omega$ and wavelength λ is given by (see Appendix A for values of physical constants)

$$\boxed{\hbar\omega \cdot \lambda = hc = 1239.842 \text{ eV nm}} \tag{1.1}$$

[‡] Numerically $a_0 = 4\pi\epsilon_0\hbar^2/me^2 = 0.529$ Å, where m is the electron rest mass, e the electron charge, ϵ_0 the permittivity of free space, and $\hbar$ Planck's constant divided by 2π. See Eisberg and Resnick, Ref. 5, for a discussion of Bohr's model of the hydrogen atom (Chapter 4) through a discussion of wave mechanics for the multi-electron atom (Chapter 10). Also see Tipler and Llewelyn, Ref. 6, for a somewhat more introductory presentation.

[¶] In multi-electron atoms the inner shells typically have very small radii, of order a_0/Z, as they experience nearly the full Coulomb attraction of the higher-Z nucleus, with little shielding by the outer electrons. A few outer electrons typically orbit with a radius na_0. See Eisberg and Resnick, Ref. 5.

[§] The phase velocity of EUV and soft x-ray radiation is derived from Maxwell's equations in Chapters 2 and 3, for propagation in vacuum and materials.

The number of photons required for one joule of energy, with wavelength given in nanometers (nm), is

$$\boxed{1 \text{ joule} \Rightarrow 5.034 \times 10^{15} \lambda[\text{nm}] \text{ photons}} \tag{1.2a}$$

or in terms of powers

$$\boxed{1 \text{ watt} \Rightarrow 5.034 \times 10^{15} \lambda[\text{nm}] \frac{\text{photons}}{\text{s}}} \tag{1.2b}$$

where 1 nm = 10 Å. Thus for a wavelength $\lambda = 1$ nm, a power of one watt corresponds to a photon flux of 5.034×10^{15} photons/s, each photon having an energy $E \simeq 1240$ eV.

1.2 Basic Absorption and Emission Processes

In this section we briefly review the basic processes through which radiation interacts with matter. In Figure 1.2 we show simplified models of the atom, with point electrons in orbit around a nucleus of positive charge $+Ze$. In x-ray notation the electron orbits are labeled K, L, and M, corresponding to principal quantum numbers $n = 1$, 2, and 3, respectively. A more accurate model of the atom is discussed in the next section, but that shown in Figure 1.2 suffices for these introductory comments.

Shown in Figure 1.2(a) is a primary electron incident on a multi-electron atom, with sufficient energy to remove a core electron in a close encounter. Common nomenclature refers to the incident electron as a *primary* electron, shown as *scattered* (redirected) off at some new angle, and in this case with reduced energy E'_p, where the lost energy is used to overcome the binding energy needed to remove the core electron, now free and referred to as a *secondary* electron, and to supply kinetic energy to the electron (E_s). The core vacancy can then be filled by an electron from a higher-lying orbit, pulled by the strong nuclear potential, with the emission of a photon of characteristic energy equal to the difference between the two shells. In Figure 1.2(b), a related process, photo-ionization, is shown in which a photon of sufficient energy is absorbed by the atom, transferring the energy to an emitted *photoelectron* with a kinetic energy equal to that of the incident photon, minus the binding energy of an electron in the particular shell. As an L-shell electron is bound to the atom with less energy than a K-shell electron, it will emerge with greater kinetic energy. Electron binding energies for hydrogen through uranium are given in Appendix B, Table B.1.

In both of these ionization processes [(a) and (b)] the atom is left with a core vacancy. The atom can rearrange itself for minimal total energy by the transition of a higher-lying electron, pulled by the strong nuclear potential, to the vacancy by one of two competing processes.

In (c) the atom is shown rearranging in a process of fluorescence, in which the electron transition is accompanied by the emission of a photon of characteristic energy equal

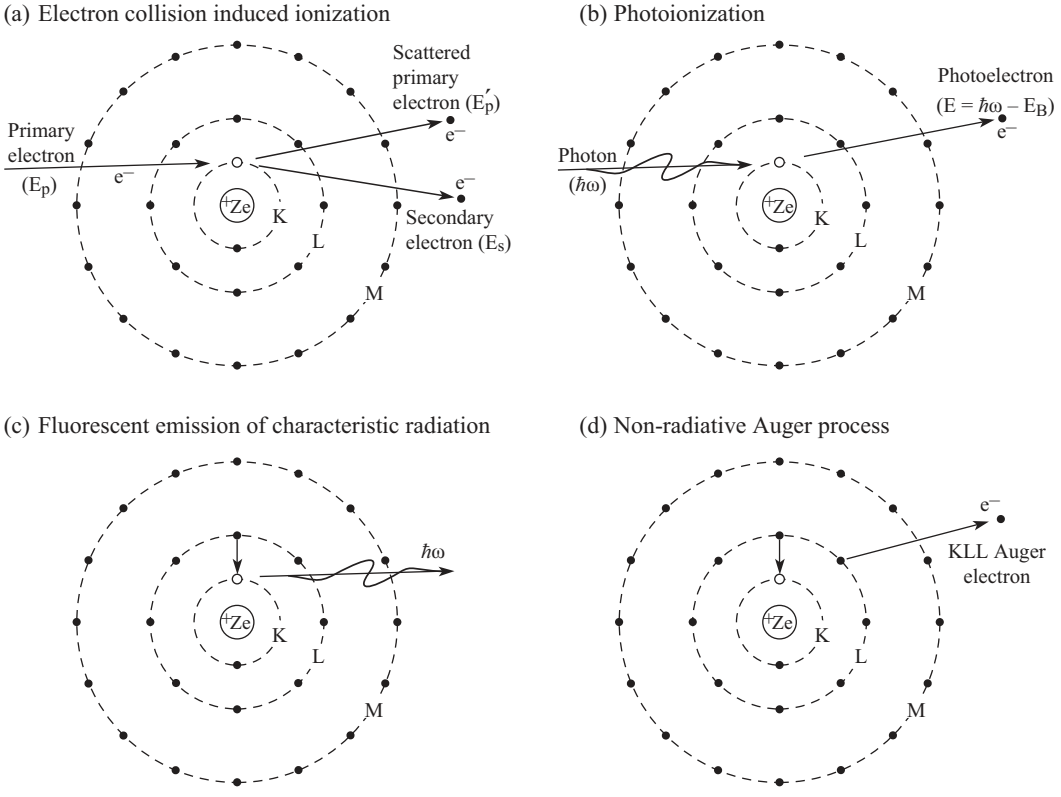

Figure 1.2 (a) An incident *primary electron* of sufficiently high energy E_p is scattered by an atom as it knocks free a core electron from the K-shell. The primary electron now travels in a new direction, with a reduced energy E_p'. The lost energy is used to overcome the binding energy of the previously bound electron, and to impart kinetic energy to what is now referred to as a *secondary electron*. The core vacancy (K-shell in this case) can then be filled by a higher-lying L- or M-shell electron. (b) An incident photon of sufficient energy $\hbar\omega$ is absorbed by the atom with the emission of a *photoelectron* of kinetic energy equal to the photon energy minus the binding energy. Again a vacancy is created, eventually to be filled by an outer electron. (c) An atom with a core vacancy readjusts as a higher-lying electron makes a transition to the vacancy, with the emission of a photon of characteristic energy (fluorescent radiation). (d) The atom adjusts to the core vacancy through the non-radiative Auger process in which one electron makes a transition to the core vacancy, while a second electron of characteristic energy is emitted. The second electron is not necessarily emitted from the same shell.

to the difference between that of the initial and final atomic states. Characteristic emission energies are given in Appendix B, Table B.2. In a competing effect (d) the atom rearranges through the emission of a second *Auger* (pronounced ō –′zhā), electron, again of characteristic energy. The emitted Auger electron is labeled with three capital letters, the first representing the shell of the original vacancy, the second representing the shell from which the vacancy is filled, and the third representing the shell from which the Auger electron is ejected. In the competition between fluorescent emission and the Auger process, the probability tends to favor fluorescence for high Z atoms, as shown

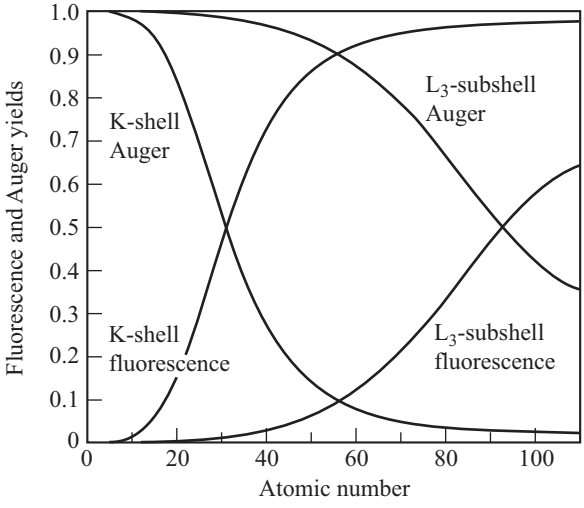

Figure 1.3 Fluorescence and Auger yields for the K-shell and the L_3-subshell as a function of atomic number Z. The Auger yields include all non-radiative contributions. Following M. Krause,[9] Oak Ridge National Laboratory.

in Figure 1.3, and the Auger process for low Z atoms.[9] Auger electron energies[9] for lithium through uranium are given in Appendix B, Table B.3. As the Auger electrons have a fixed characteristic energy, they are used extensively for elemental characterization in surface and interface analysis.

The study of atoms, molecules, and surfaces by the measurement of photoelectron kinetic energies, as a function of incident photon energy, is known as photoemission spectroscopy.[10] This process is widely used for the elemental identification and analysis of chemical bonding for atoms at or near surfaces. As generally employed, photons of fixed energy penetrate a surface or thin film, providing the energy required to lift bound electrons into the continuum, as shown in Figure 1.4. With well-known electron binding energies (Appendix B, Table B.1) the observed kinetic energies can be used to identify the elements present. As the binding energies of core electrons are affected by the orbital parameters of the outer electrons (chemical bonding in molecules, valence and conduction bands in solids), photoemission also provides a powerful tool for the study of chemical states.[11–17] As L-shell energies are more sensitive to the bonding of outer electrons than are the energies of the more tightly bound and shielded K-shell electrons, the L-shell electrons are more commonly used in photoemission studies.

If the emitted photoelectron travels any distance in a material, it is likely to lose energy quickly through interactions with other electrons (individual collisions or collective motion). Figure 1.5 shows typical electron range data, as a function of electron energy, in aluminum and gold,[18] as well as a *universal curve* for many materials.[19, 20] With incident photon energies characteristic of the EUV/soft-x-ray spectral region, it is clear that photoelectron ranges will be extremely short, of order 1 nm, so that these techniques are clearly limited to surface science.

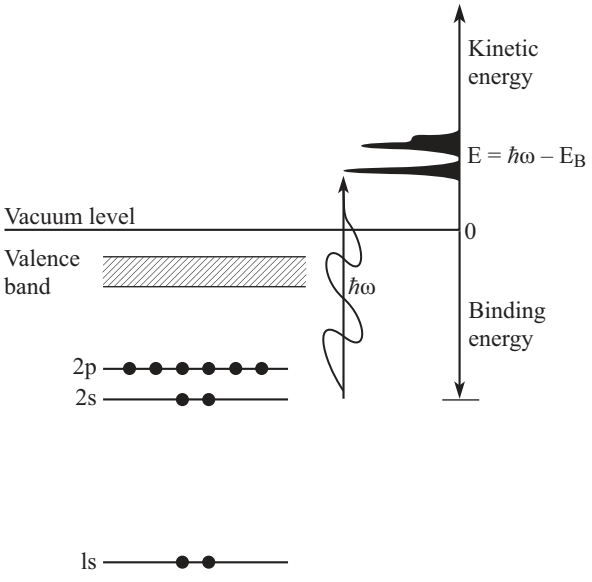

Figure 1.4 The process of photoemission in which an absorbed photon transfers its energy to a bound electron near the material–vacuum interface, resulting in a transition to a free electron state in the continuum with kinetic energy (E) equal to that of the incident photon ($\hbar\omega$) minus the binding energy (E_B).

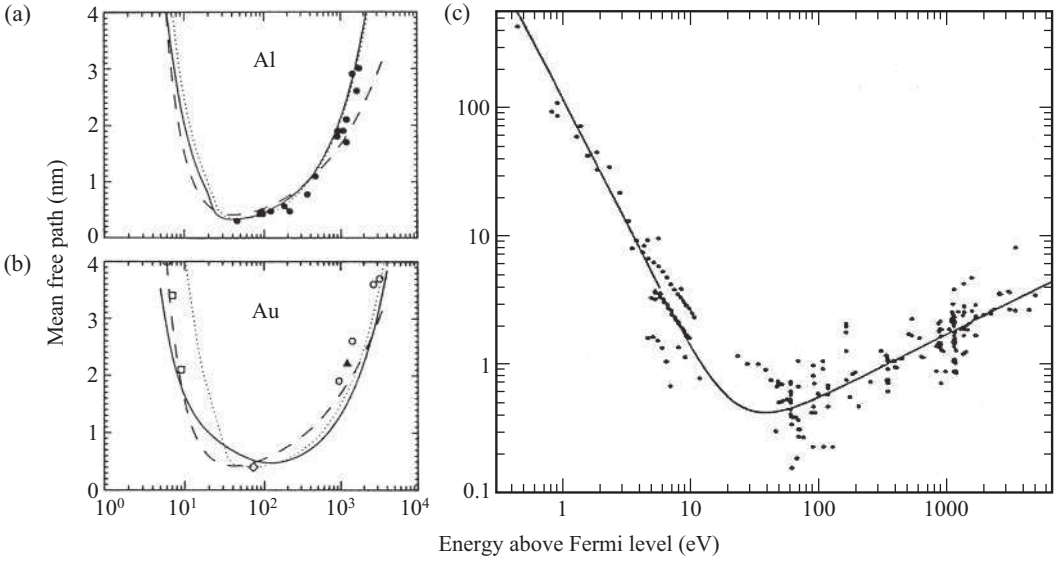

Figure 1.5 Electron mean free path, as a function of electron energy, for (a) aluminum, (b) gold, and (c) a combination of many materials. The data in (a) and (b) are from Penn,[18] while the data in (c) are from Seah and Dench.[19] The various curves reflect efforts to develop a universal model that describes inelastic scattering of electrons in a solid.

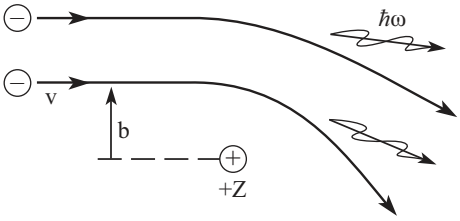

Figure 1.6 Bremsstrahlung radiation occurs predominantly when an incident electron is accelerated as it passes a nucleus, causing it to radiate. A broad continuum of radiation results when a large number of electrons interact randomly with nuclei at various distances of closest approach, *b*, resulting in wide variations in experienced acceleration and collision time.

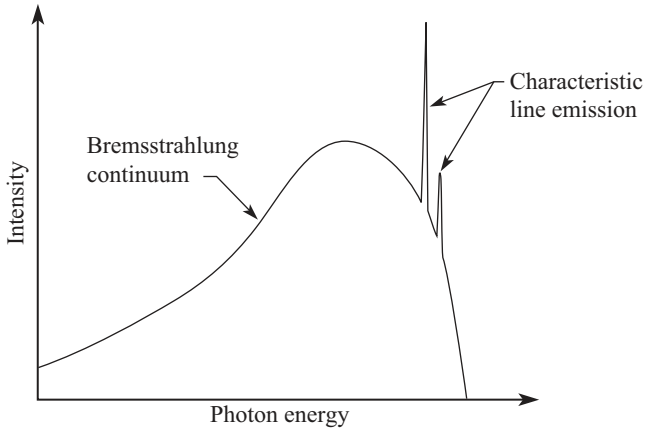

Figure 1.7 Continuum radiation and narrow line emission from a solid target as might be observed as cathode electrons strike the anode in an electrical discharge tube.

When observing the emission spectrum from a solid material bombarded by electrons it is typical to observe both characteristic line emission and continuum emission. This latter process is called *bremsstrahlung*, from the German word for "braking radiation." Figure 1.6 shows a simple diagram of the process, in which electrons of a given velocity v, or energy *E*, approach an electron or nucleus at various distances of closest approach, *b* (the *impact parameter*), experiencing a wide range of accelerations (depending on the closeness of the interaction) and thus emitting photons across a wide range of energies. With a large number of incident electrons and a wide variety of impact parameters, a rather broad continuum of radiation is produced. Where photoemission occurs due to direct impact with bound electrons, as described earlier in Figure 1.2(a), characteristic line emission is also observed. Both phenomena are illustrated, as they might typically be observed,[21] in Figure 1.7. The nature and nomenclature of the characteristic line emissions are discussed in the following section.

Historically, the process of photoabsorption [Figure 1.2(b)] has been observed macroscopically by passing radiation through thin foils and observing the resultant decrease in intensity as a function of thickness.[22] As shown in Figure 1.8, one observes that with

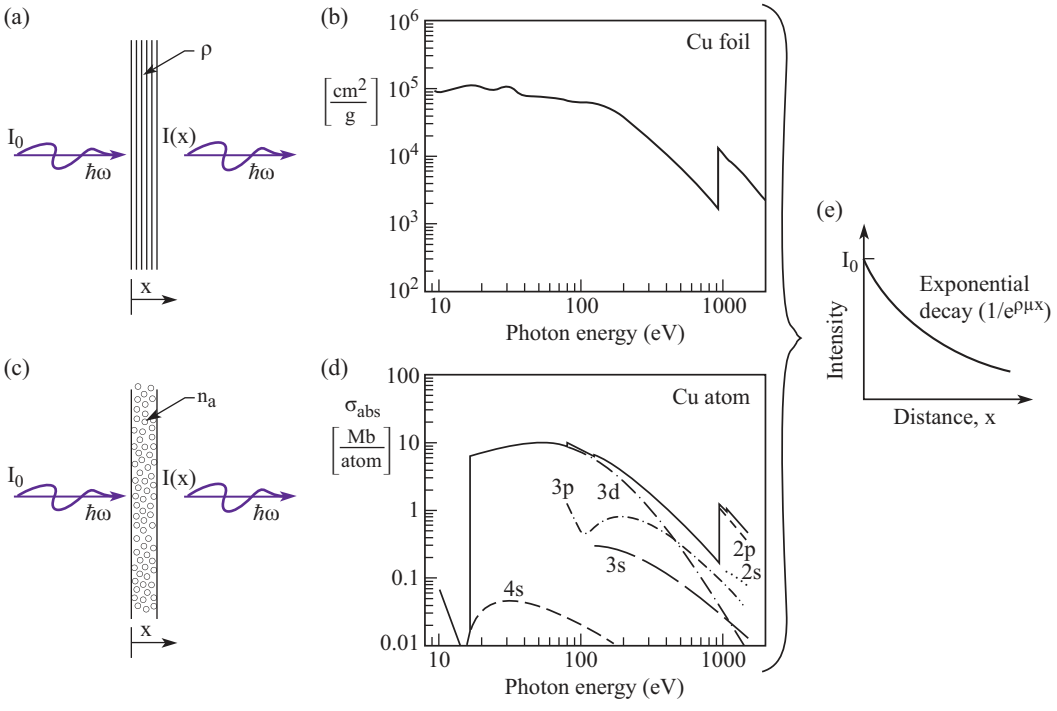

Figure 1.8 (a) Photoabsorption as observed with thin foils of increasing thickness x at fixed photon energy, with (b) an example of the linear absorption coefficient μ for copper (from Henke, Gullikson, and Davis[3]). The same process is described on an atomic level in (c), with the photoabsorption cross-section (photoionization) for a copper atom in (d) (from Yeh and Lindau[4]). Exponential attenuation of the radiation is shown in (e). Differences observed in comparing (b) and (d) are due to solid state effects in metallic copper foils, most noticeably for copper in the absence of the atomic 3d edge just above 10 eV photon energy.

incremental increases in thickness, Δx, there is an an incremental decrease in transmitted intensity I, relative to the incident intensity I_0, such that

$$\frac{\Delta I}{I_0} = -\rho\mu\ \Delta x$$

where ρ is the mass density and μ is an energy- and material-dependent absorption coefficient. Writing this in the differential limit ($\Delta x \to dx$, $\Delta I \to dI$), the equation integrates to a logarithmic dependence $\ln(I/I_0) = -\rho\mu x$, or in exponential form

$$\boxed{\frac{I}{I_0} = e^{-\rho\mu x}} \tag{1.3a}$$

where $\mu = \mu(E, Z)$, $E = \hbar\omega$ is the photon energy, Z represents the elemental dependence, and μ is the *linear absorption coefficient*. Standard values of μ are given in Appendix C